European Review for Medical and Pharmacological Sciences 2022; 26: 432-439

MicroRNA-18-5p inhibits the oxidative stress and apoptosis of myocardium induced by hypoxia by targeting RUNX1

P. LI[1], X.-Y. JIA[2]

[1]Department of Emergency Medicine, Beijing Chao-Yang Hospital, Capital Medical University, Beijing, China
[2]Basic laboratory, Beijing Chao-Yang Hospital, Capital Medical University, Beijing, China

Abstract. – OBJECTIVE: Acute myocardial infarction (AMI) is the main cause of sudden death in the world. The aim of this paper was to explore the role of microRNA-18-5p (miR-18-5p) in myocardial infarction (MI) and its potential mechanism.

MATERIALS AND METHODS: The expression of miRNA and protein was detected using quantitative reverse-transcription polymerase chain reaction (RT-PCR) analysis and Western blot. The level of oxidative stress of cardiomyocytes was evaluated by detecting the contents of Superoxide dismutase (SOD), Reactive oxygen species (ROS) and Malondialdehyde (MDA). Caspase-3 activity assay, flow cytometry and TUNEL staining were employed to evaluate apoptosis of myocardium. Dual-Luciferase reporter gene assay was used to prove whether miR-18-5p targeted RUNX1.

RESULTS: MiR-18-5p was down-regulated in hypoxia-treated H9c2 cells. Hypoxia treatment induced oxidative stress and apoptosis of H9c2 cells. The oxidative stress of H9c2 was manifested by the decrease of SOD activity, the increase of ROS and MDA levels, and the apoptosis of H9c2 was shown by the increase of caspase-3 activity and apoptosis rate. MiR-18-5p mimic was transfected into H9c2 cells and successfully up-regulated miR-18-5p. And overexpression of miR-18-5p markedly inhibited the oxidative stress and apoptosis caused by hypoxia in H9c2 cells. Through bioinformatics analysis and Dual-Luciferase reporter gene assay, RUNX1 was proved to have binding sites for miR-18-5p. Furthermore, knocking down RUNX1 using small interfering RNA-RUNX1 (siR-RUNX1) significantly protected H9c2 cells from oxidative stress and apoptosis.

CONCLUSIONS: MiR-18-5p expression was decreased in hypoxia-treated H9c2 cells. Overexpression of miR-18-5p alleviated hypoxia-induced oxidative stress and apoptosis in H9c2 cells via targeting RUNX1.

Key Words:
Acute myocardial infarction, MicroRNA-18-5p, Apoptosis, Oxidative stress, RUNX1.

Introduction

Acute myocardial infarction (AMI) is one of the common types of coronary heart disease (CHD) in clinic. Its morbidity, mortality and disability rate are high, and it has become a serious threat to human health[1,2]. Current clinical treatment methods include drug thrombolysis, coronary intervention and coronary artery bypass grafting[3,4]. Although these treatments have benefited more and more patients and the mortality rate has decreased significantly, due to poor regeneration of myocardial cells after infarction, the heart cannot be repaired by regeneration of myocardial cells. The loss of myocardial cells after myocardial infarction (MI) and the subsequent ventricular remodeling are the main causes of a series of complications after MI, especially heart failure, which affects the prognosis of patients. How to promote the repair and functional reconstruction of myocardial cells in the area of necrosis after MI and prevent ventricular remodeling has become the key to improving the prognosis of patients with MI.

MicroRNA (miRNA) participates in post-transcriptional gene expression regulation by inducing target gene silencing. In mammals, the exact match between the "seed sequence" of the 2nd to 8th nucleotides at the 5' end of the miRNA sequence and the target mRNA 3'-untranslated region (3'UTR) is the basis of miRNA negative regulation[5-7]. A miRNA can inhibit multiple different protein-coding genes, and a specific protein-coding gene can be regulated by multiple different miRNAs. This complex regulatory network can regulate the expression of multiple genes through a miRNA or can finely regulate the expression of a gene through the combination of several miRNAs. Abnormal expression of miRNA is closely related to the pathophysiological processes of var-

Corresponding Author: Xingyuan Jia, Ph.D; e-mail: jiax@ccmu.edu.cn

ious cardiovascular diseases[8]. MiR-34a silencing has been shown to inhibit cardiac aging and myocardial cell death and fibrosis after MI[9]. Chu et al[10] showed that miR-130 could aggravate myocardial injury after MI *via* targeting PPAR-γ. However, the role of miR-18-5p in MI has not been studied.

In this study, we established MI model *in vitro* to detected miR-18-5p expression. Moreover, the role of miR-18-5p in MI was studied by up-regulation of miR-18-5p. Our results suggested that miR-18-5p could become a potential therapeutic target for MI.

Materials and Methods

Cell Culture

The complete medium for cultivating H9c2 cells (Invitrogen, Carlsbad, CA, USA) was formulated with 3 ingredients: Dulbecco's Modified Eagle's Medium (DMEM) (Gibco, Rockville, MD, USA), 10% fetal bovine serum (FBS) (Gibco, Rockville, MD, USA) and 1% penicillin/streptomycin (Gibco, Rockville, MD, USA). The cell incubator that cultivated H9c2 cells maintained a constant temperature of 37°C and contained 5% CO_2. To establish a cell model of MI, H9c2 cells were placed in a cell incubator containing 5% CO_2 and 1% O_2 for 12 hours.

Transfection of MiRNA Mimic and siRNA

MiR-18-5p mimic, mimic negative control (NC), small interfering RNA-RUNX1 (siR-RUNX1), and siR-NC were produced and designed by RiboBio (Guangzhou, China). These synthetic RNAs were transfected into H9c2 cells using the Transfection Kit (RiboBio, Guangzhou, China) according to the instructions.

Quantitative Reverse-Transcription Polymerase Chain Reaction (RT-PCR) Analysis

After washing the H9c2 cells with pre-chilled phosphate-buffered saline (PBS) 3 times, we added 1.0 mL of TRIzol reagent (Invitrogen, Carlsbad, CA, USA) to each well, and mixed thoroughly to obtain a cell suspension. The cell suspension was transferred to a 1.5 mL Eppendorf (EP) tube. After the cell suspension was allowed to stand at room temperature for 5 minutes, 0.2 ml of chloroform was added, and the mixture was shaken vigorously for 30 seconds and allowed to stand for 5 minutes. Then, the mixture was centrifuged at 12000 rpm and 4°C for 15 minutes, and the upper colorless aqueous phase was carefully transferred to another new 1.5 mL EP tube. An equal volume of isopropanol was added, and the mixture was gently inverted. After standing at room temperature for 10 minutes, it was centrifuged at 12000 rpm and 4°C for 15 minutes. Subsequently, the supernatant was discarded, and the RNA was washed with 75% ethanol and then precipitated by centrifugation at 7500 g at 4°C for 10 minutes. The RNA pellet was dried in air for 5 minutes. 30 μL of diethyl pyrocarbonate (DEPC)-treated Water (Beyotime, Shanghai, China) was used to dissolve RNA and then stored in a refrigerator at -80°C. 1 μL of total RNA sample was used to determine the RNA concentration and purity on the NanoDrop 2000 ultramicro spectrophotometer. The purity of RNA samples was judged by the absorbance ratio of RNA samples at wavelengths of 260 nm and 280 mn, with A260/280 in the range of 1.8-2.0 being the best. According to the instructions of All-in-One™ miRNA First-Strand complementary deoxyribose nucleic acid (cDNA) Synthesis Kit (GeneCopoeia, Guangzhou, China), the total RNA extracted was used for specific reverse transcription of miR-18-5p. All-in-One™ miRNA qPCR Kit (GeneCopoeia, Guangzhou, China) was used for miR-18-5p amplification. U6 was the internal control of miR-18-5p. All the primers were listed in Table I.

Cell Counting Kit-8 (CCK-8) Assay

The viability of H9c2 cells was measured using CCK-8 Cell Counting Kit (Vazyme, Nanjing, China). 10 μL CCK-8 solution was added to each well. The absorbance at 450 nm was measured using a microplate reader.

Reactive Oxygen Species (ROS) Quantification

The levels of ROS in H9c2 cells were measured using DHR-ROS test kit (Bestbio, Shanghai, China) in accordance with protocols.

Superoxide Dismutase (SOD) Activity Assay

The SOD levels in H9c2 cells were detected using SOD Assay Kit (KeyGen, Shanghai, China) in accordance with the protocols.

Malondialdehyde (MDA) Levels

The MDA levels in cell supernatant were detected using Lipid Peroxidation MDA Assay Kit (Beyotime, Shanghai, China) according to the protocols.

Table I. Real time PCR primers.

Gene name	Forward (5'>3')	Reverse (5'>3')
miR-18-5p	AGGCGTAAGGTGCATCTAG	AACAACCAACACAACCCAAC
U6	CTCGCTTCGGCAGCACA	AACGCTTCACGAATTTGCGT

RT-PCR, quantitative reverse-transcription polymerase chain reaction.

Caspase-3 Activity

Caspase-3 activity of H9c2 cells was detected by Caspase-3 activity detection kit (Beyotime, Shanghai, China) according to the protocols.

Flow Cytometry

The apoptosis rate of H9c2 cells was detected using Annexin V-FITC/PI Apoptosis Detection Kit (Vazyme, Nanjing, China). After collecting cells of each group by digestion with trypsin, the cells were washed twice with pre-chilled PBS buffer. After centrifugation at 2000 rpm for 10 min, 100 μL of Binding Buffer was added to re-suspend the cells. 100 μL of the cell suspension was transferred to a flow tube, 5 μL of Annexin V-FITC and PI staining solution were added, and after careful mixing, the reaction was carried out at room temperature in the dark for 15 minutes. After each tube was supplemented with 400 μL of Binding Buffer, the flow cytometer was used to detect Annexin V-FITC and PI signals on the machine to statistically analyze the apoptosis rate of each group.

TUNEL Staining

The apoptosis of H9c2 cells was detected using TUNEL BrightRed Apoptosis Detection Kit (Vazyme, Nanjing, China) as instructed by the manufacturer. The nucleus was stained with DAPI (Beyotime, Shanghai, China). TUNEL staining was observed by a fluorescence microscope.

Western Blot

Total protein of H9c2 cells was obtained using radioimmunoprecipitation assay (RIPA) lysis buffer (Beyotime, Shanghai, China). Protein concentration was measured using the bicinchoninic acid (BCA) method (Beyotime, Shanghai, China). 30 μg of protein was loaded and electrophoresed on sodium dodecyl sulphate-polyacrylamide gel electrophoresis (SDS-PAGE) gel at a constant voltage of 120 V. After electrophoresis was completed, the separated proteins were transferred to the polyvinylidene difluoride (PVDF) membrane (Millipore, Billerica, MA, USA) with a constant current of 300 mA. The membrane was then incubated in 5% skim milk to block non-specific antigens. 2 hours later, the membrane was incubated in the primary antibody (RUNX1, Abcam, Cambridge, MA, USA: Rabbit, 1:1000; GAPDH, Abcam, Cambridge, MA, USA Rabbit, 1:1000) overnight. Then secondary antibody was employed to incubate the membranes for 2 hours. Finally, Super enhanced chemiluminescence (ECL) Detection Reagent (YEASEN, Shanghai, China) was used to develop the blots in Image Lab™ Software.

Luciferase Activity Assay

Luciferase reporter plasmids (RiboBio, Guangzhou, China) containing wild-type (WT) or mutant (MUT) 3'UTR of RUNX1 were constructed. MiR-18-5p mimic or NC along with Luciferase reporter plasmids were co-transfected into HEK293T cells. According to the instructions of the Dual-Luciferase Reporter Assay System kit (RiboBio, Guangzhou, China), the firefly Luciferase and Renilla Luciferase activities of the cells in each group after transfection were measured.

Statistical Analysis

Measurement data were expressed as $\chi \pm s$, and the measurement data were tested for normality. Differences between two groups were analyzed by using the Student's *t*-test. Comparison between multiple groups was done using One-way ANOVA test followed by Post-Hoc Test (Least Significant Difference). Test level $\alpha=0.05$.

Results

MiR-18-5p Was Down-Regulated in Hypoxia-Treated H9c2 Cells

To explore the appropriate time for the establishment of MI cell model using hypoxia treatment, we measured the viability of H9c2 cells un-

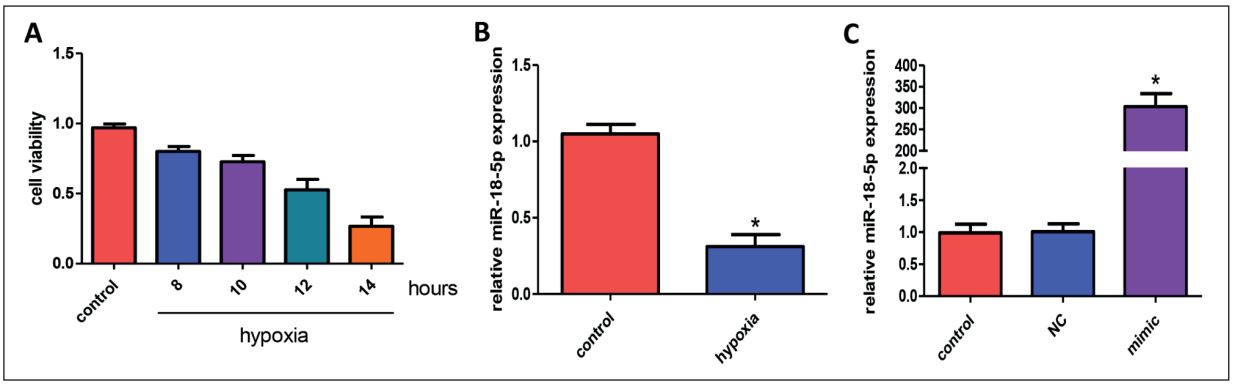

Figure 1. MiR-18-5p was down-regulated in hypoxia-treated H9c2 cells. **A**, The viability of H9c2 cells treated with hypoxia was detected using CCK-8 assay. **B**, MiR-18-5p expression in H9c2 cells was detected by RT-PCR ("*" $p<0.05$ *vs.* control, n = 3). **C**, Transfection of miR-18-5p mimic into H9c2 cells significantly increased miR-18-5p expression ("*" $p<0.05$ *vs.* NC, n = 3).

der different periods of hypoxia. As can be seen from Figure 1A, the cell viability of H9c2 cells decreased by about 50% after 12 hours of hypoxia, so we chose 12 hours of hypoxia to build a MI cell model. Afterwards, by RT-PCR, we found that miR-18-5p expression decreased significantly in cardiomyocytes treated with hypoxia (Figure 1B). To further study the function of miR-18-5p, miR-18-5p was overexpressed using miR-18-5p mimic (Figure 1C).

Up-Regulation of MiR-18-5p Inhibited Hypoxia-Induced Oxidative Stress and Apoptosis of H9c2 Cells

After H9c2 cells were treated with hypoxia, the expression of SOD decreased greatly, while the levels of ROS and MDA increased markedly, suggesting that hypoxia induced oxidative stress in H9c2 cells. After overexpression of miR-18-5p, the oxidative stress of H9c2 cells was remarkably inhibited (Figure 2A-2C). In addition, hypoxia treatment also induced the apoptosis of H9c2 cells, which was manifested by the increased expression of Caspase-3 and the increased apoptosis rate. However, up-regulation of miR-18-5p protected H9c2 cells from hypoxia-induced apoptosis (Figure 2D-2F).

MiR-18-5p Directly Targets RUNX1

Through the TargetScan database, RUNX1 was predicted to be the target gene of miR-18-5p (Figure 3A). Moreover, overexpression of miR-18-5p notably inhibited RUNX1 expression (Figure 3B). Further, overexpression of miR-18-5p significantly inhibited the activity of Luciferase, proving that miR-18-5p directly targets RUNX1 mRNA (Figure 3C).

Knockdown of RUNX1 Inhibited Hypoxia-Induced Oxidative Stress and Apoptosis of H9c2 Cells

To prove whether RUNX1 can regulate hypoxia-induced oxidative stress and apoptosis in H9c2 cells, we silenced RUNX1 by transfecting siR-RUNX1 into cells. Silencing RUNX1 increased the expression of SOD in H9c2 cells and inhibited the production of ROS and MDA (Figure 4A-4C). These proved the anti-oxidative stress of silencing RUNX1 on cardiomyocytes. In addition, silencing RUNX1 inhibited the activity of Caspase-3 in H9c2 cells and significantly reduced the rate of apoptosis, as evidenced by flow cytometry and TUNEL staining (Figure 4D-4F). These results demonstrate the anti-cardiomyocyte apoptosis effect of silencing RUNX1.

Discussion

In this present study, we revealed the role of miR-18-5p in MI. We have revealed for the first time that miR-18-5p is down-regulated in MI. Overexpression of miR-18-5p could inhibit hypoxia-induced oxidative stress and apoptosis of myocardium. This protective effect was achieved at least in part by targeting RUNX1.

Cardiovascular disease has become prevalent with the aging of the population and the acceleration of urbanization. AMI, a major ischemic heart disease, is a grave threat to human health. AMI, especially large-area transmural MI, can lead to complex changes in the structure and function of the ventricle, including the infarcted area and

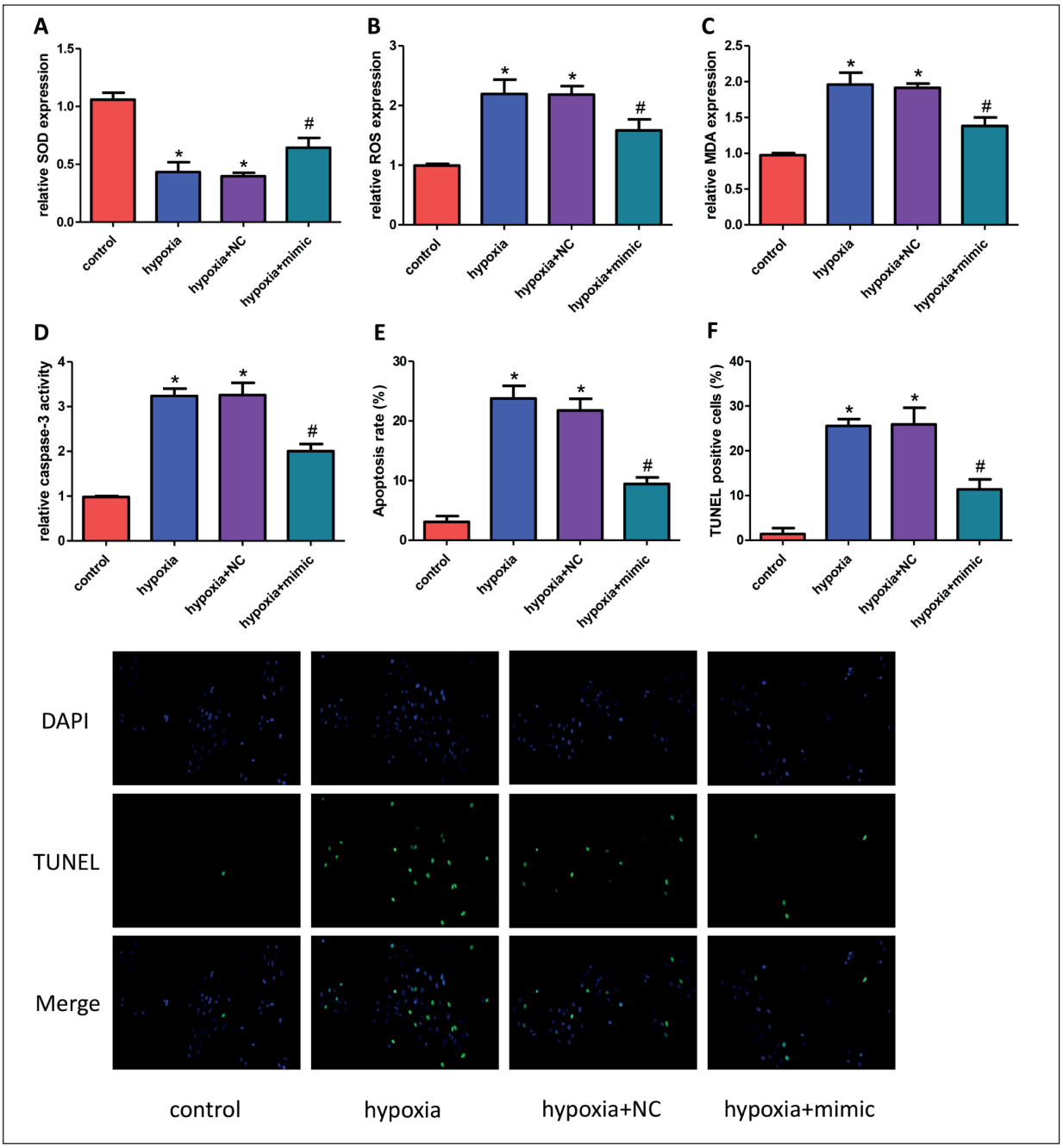

Figure 2. Up-regulation of miR-18-5p inhibited hypoxia-induced oxidative stress and apoptosis of H9c2 cells. The expression of SOD **(A)** and ROS **(B)** and MDA **(C)** in H9c2 cells ("$_{*}$" $p<0.05$ *vs.* control, "$_{\#}$" $p<0.05$ *vs.* hypoxia+NC, n=3). **D**, The Caspase-3 activity in H9c2 cells ("$_{*}$" $p<0.05$ *vs.* control, "$_{\#}$" $p<0.05$ *vs.* hypoxia+NC, n=3). **E**, Apoptosis rate was detected by flow cytometry ("$_{*}$" $p<0.05$ *vs.* control, "$_{\#}$" $p<0.05$ *vs.* hypoxia+NC, n=3). **F**, Results of TUNEL staining of H9c2 cells in each group (200×) ("$_{*}$" $p<0.05$ *vs.* control, "$_{\#}$" $p<0.05$ *vs.* hypoxia+NC, n=3).

non-infarcted area, namely ventricular remodeling. Ventricular remodeling can lead to ventricular dilation, heart failure and arrhythmia. It is one of the main factors that determine the cardiac function and prognosis of MI patients. Preventing ventricular remodeling after MI is an important link that cannot be ignored in preventing heart failure[11,12]. An important feature of ventricular remodeling is cell death. Several studies have shown that the main form of cardiomyocyte death after

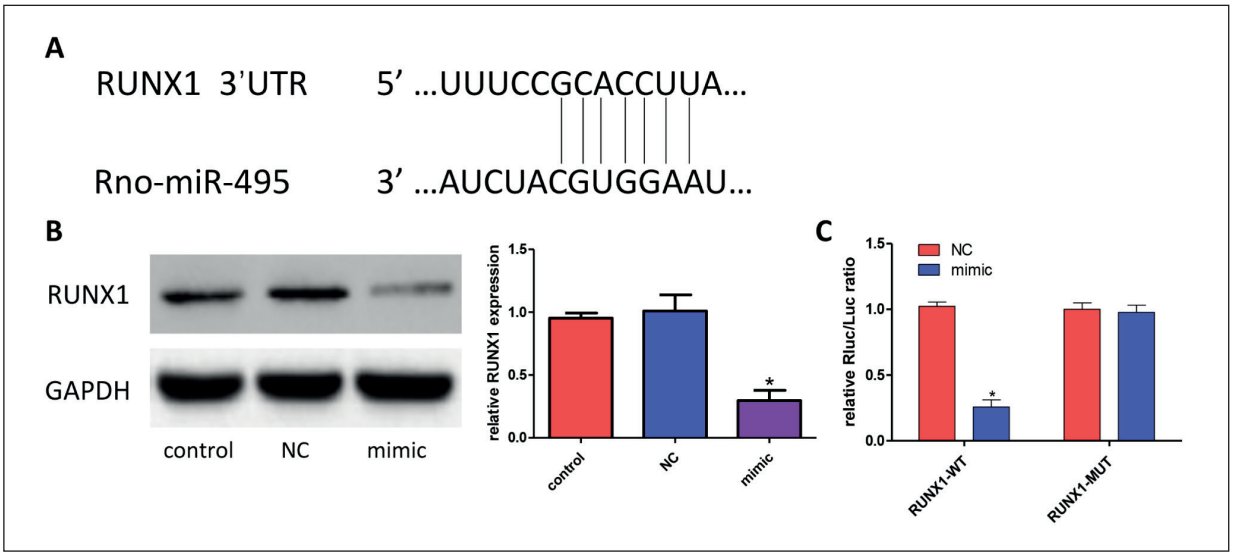

Figure 3. MiR-18-5p directly targets RUNX1. **A**, Binding site predicted by the TargetScan database. **B**, Western blot showed the expression of RUNX1 ("*" $p<0.05$ *vs.* NC, n=3). **C**, MiR-18-5p mimic significantly decreased the relative luciferase activity in RUNX1-WT group, but did not decrease the relative luciferase activity in RUNX1-MUT group ("*" $p<0.05$ *vs.* NC, n = 3).

MI is apoptosis rather than cell necrosis. Cardiomyocyte apoptosis after MI not only affects the area of MI, but causes ventricular remodeling[13,14].

Apoptosis and necrosis of myocardial tissue and cells caused by ischemia and hypoxia are important factors for the occurrence and development of MI. Existing studies have shown that there are many mechanisms involved in apoptosis, among which mitochondria are important productivity organs, and a variety of apoptotic proteins can induce mitochondria to initiate apoptosis programs. Moreover, various pathological factors can regulate intracellular Caspase-3, programmed cell death 5 (PDCD-5) and Bcl-2, Bax, and induce cell apoptosis[15-17].

Oxidative stress has been confirmed to be involved in the process of myocardial cell apoptosis after myocardial infarction. The view is that reactive oxygen species (ROS) can be used as signaling molecules to mediate apoptosis[18]. Under normal physiological conditions, low levels of ROS play an important role in signaling and metabolic pathways. However, during MI, overproduction of ROS will lead to oxidative stress, leading to DNA oxidation, initiating membrane lipid peroxidation chain reaction, changing membrane fluidity and destroying the integrity of cells, causing changes in cell function and even necrosis[19]. Excessive ROS is liable to undergo peroxidation reaction with lipid to produce MDA. MDA is the final product of lipid peroxidation reaction, so MDA is often used as an index to evaluate the degree of ROS. And SOD is the main antioxidant enzyme, which can effectively eliminate free radicals in the body[20,21].

RUNX1 (Runt-related transcription factor 1) has been shown to participate in the regulation of various biological processes, such as cell proliferation and apoptosis. Li et al[22] proved that miR-101 could alleviate myocardial injury after MI and improve cardiac function of MI rats *via* targeting RUNX1.

In this paper, we construct a cell model of MI by hypoxia treatment. Moreover, hypoxia treatment induced oxidative stress and apoptosis of H9c2 cells. By RT-PCR, miR-18-5p was found to be down-regulated in H9c2 cells treated with hypoxia. The overexpression of miR-18-5p significantly inhibited the oxidative stress and apoptosis of H9c2 cells. Through bioinformatics analysis and Luciferase reporter gene experiments, we demonstrated that miR-18-5p directly targets RUNX1. And knocking down RUNX1 can significantly protect H9c2 cells from hypoxia-induced oxidative stress and apoptosis.

Conclusions

MiR-18-5p was down-regulated in MI. Up-regulation of miR-18-5p could inhibit myocardial oxidative stress and apoptosis induced by hypoxia *via* targeting RUNX1.

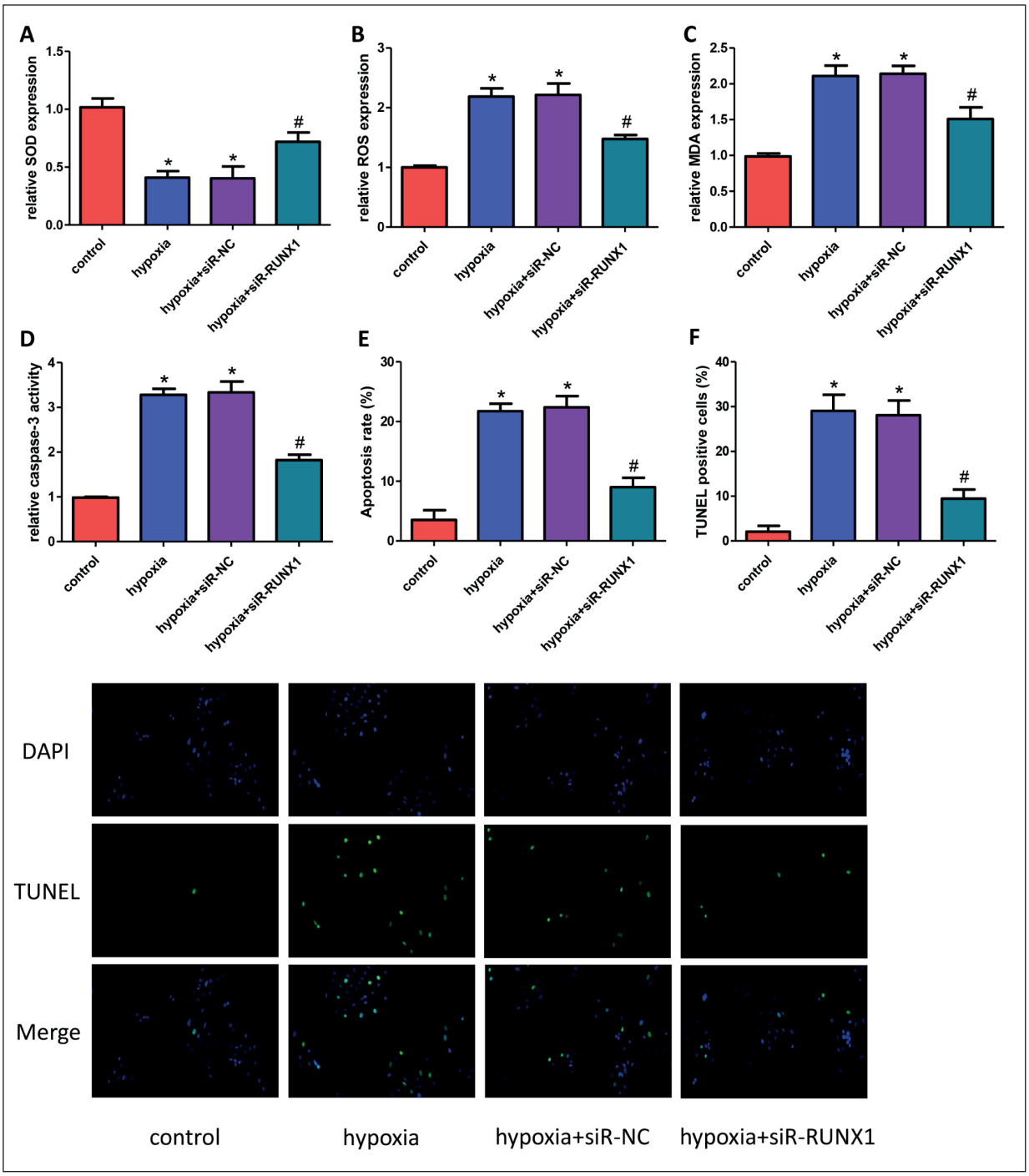

Figure 4. Knockdown of RUNX1 inhibited hypoxia-induced oxidative stress and apoptosis of H9c2 cells. The expression of SOD **(A)** and ROS **(B)** and MDA **(C)** in H9c2 cells ("$_{*}$" $p<0.05$ *vs.* control, "$_{\#}$" $p<0.05$ *vs.* hypoxia+siR-NC, n=3). **D**, The Caspase-3 activity in H9c2 cells ("$_{*}$" $p<0.05$ *vs.* control, "$_{\#}$" $p<0.05$ *vs.* hypoxia+siR-NC, n=3). **E**, Apoptosis rate was detected by flow cytometry ("$_{*}$" $p<0.05$ *vs.* control, "$_{\#}$" $p<0.05$ *vs.* hypoxia+siR-NC, n=3). **F**, Results of TUNEL staining of H9c2 cells in each group (200×) ("$_{*}$" $p<0.05$ *vs.* control, "$_{\#}$" $p<0.05$ *vs.* hypoxia+siR-NC, n=3).

Conflict of Interests

The authors declare that they have no conflict of interests.

References

1) Wartenberg KE. Malignant middle cerebral artery infarction. Curr Opin Crit Care 2012; 18: 152-163.
2) Boateng S, Sanborn T. Acute myocardial infarction. Dis Mon 2013; 59: 83-96.
3) Lu L, Liu M, Sun R, Zheng Y, Zhang P. Myocardial Infarction: Symptoms and Treatments. Cell Biochem Biophys 2015; 72: 865-867.
4) Anderson JL, Morrow DA. Acute Myocardial Infarction. N Engl J Med 2017; 376: 2053-2064.
5) Meijer HA, Smith EM, Bushell M. Regulation of miRNA strand selection: follow the leader? Biochem Soc Trans 2014; 42: 1135-1140.
6) Afonso-Grunz F, Muller S. Principles of miRNA-mRNA interactions: beyond sequence complementarity. Cell Mol Life Sci 2015; 72: 3127-3141.
7) Fabian MR, Sonenberg N. The mechanics of miRNA-mediated gene silencing: a look under the hood of miRISC. Nat Struct Mol Biol 2012; 19: 586-593.
8) Wojciechowska A, Braniewska A, Kozar-Kaminska K. MicroRNA in cardiovascular biology and disease. Adv Clin Exp Med 2017; 26: 865-874.
9) Boon RA, Iekushi K, Lechner S, Seeger T, Fischer A, Heydt S, Kaluza D, Treguer K, Carmona G, Bonauer A, Horrevoets AJ, Didier N, Girmatsion Z, Biliczki P, Ehrlich JR, Katus HA, Muller OJ, Potente M, Zeiher AM, Hermeking H, Dimmeler S. MicroRNA-34a regulates cardiac ageing and function. Nature 2013; 495: 107-110.
10) Chu X, Wang Y, Pang L, Huang J, Sun X, Chen X. miR-130 aggravates acute myocardial infarction-induced myocardial injury by targeting PPAR-gamma. J Cell Biochem 2018; 119: 7235-7244.
11) Willenheimer R. Left ventricular remodelling and dysfunction. Can the process be prevented? Int J Cardiol 2000; 72: 143-150.
12) Hashimoto H, Olson EN, Bassel-Duby R. Therapeutic approaches for cardiac regeneration and repair. Nat Rev Cardiol 2018; 15: 585-600.
13) Palojoki E, Saraste A, Eriksson A, Pulkki K, Kallajoki M, Voipio-Pulkki LM, Tikkanen I. Cardiomyocyte apoptosis and ventricular remodeling after myocardial infarction in rats. Am J Physiol Heart Circ Physiol 2001; 280: H2726-H2731.
14) Konstam MA, Kramer DG, Patel AR, Maron MS, Udelson JE. Left ventricular remodeling in heart failure: current concepts in clinical significance and assessment. JACC Cardiovasc Imaging 2011; 4: 98-108.
15) Frangogiannis NG. Pathophysiology of Myocardial Infarction. Compr Physiol 2015; 5: 1841-1875.
16) Burke AP, Virmani R. Pathophysiology of acute myocardial infarction. Med Clin North Am 2007; 91: 553-572.
17) Anversa P, Cheng W, Liu Y, Leri A, Redaelli G, Kajstura J. Apoptosis and myocardial infarction. Basic Res Cardiol 1998; 93 Suppl 3: 8-12.
18) Carmody RJ, Cotter TG. Signalling apoptosis: a radical approach. Redox Rep 2001; 6: 77-90.
19) Sokolova N, Pan S, Provazza S, Beutner G, Vendelin M, Birkedal R, Sheu SS. ADP protects cardiac mitochondria under severe oxidative stress. PLoS One 2013; 8: e83214.
20) Choudhary R, Bodakhe SH. Magnesium taurate prevents cataractogenesis via restoration of lenticular oxidative damage and ATPase function in cadmium chloride-induced hypertensive experimental animals. Biomed Pharmacother 2016; 84: 836-844.
21) Kashka RH, Zavareh S, Lashkarbolouki T. Augmenting effect of vitrification on lipid peroxidation in mouse preantral follicle during cultivation: modulation by coenzyme Q10. Syst Biol Reprod Med 2016; 62: 404-414.
22) Li X, Zhang S, Wa M, Liu Z, Hu S. MicroRNA-101 protects against cardiac remodeling following myocardial infarction via downregulation of runt-related transcription factor 1. J Am Heart Assoc 2019; 8: e13112.